Received: Added at production | Revised: Added at production | Accepted: Added at production

DOI: xxx/xxxx

ARTICLE TYPE

Analysis and Control of a Multi-layer Time-Varying SIS Model with an Infrastructure Network †

Sebin Gracy*[1] | Jesse Wayment[2] | Irinel C. Morărescu[3] | Vineeth S. Varma[3] | Philip E. Paré[2]

[1]Department of Electrical Engineering and Computer Science, South Dakota School of Mines and Technology, Rapid City, SD, USA

[2]Elmore Family School of Electrical and Computer Engineering, Purdue University, West Lafayette, IN, USA

[3]CRAN, Université de Lorraine, CNRS, Grand Est, France

Correspondence

*Sebin Gracy,

Email: sebin.gracy@sdsmt.edu

Summary

The article studies multi-competitive continuous-time epidemic processes across a network consisting of individuals in one layer and shared resources in the other layer. The digraph representing the interconnection between the individuals may be time-varying. The introduction of multiple shared resources in the infrastructure network adds to the complexity, as the susceptible individuals can be infected by not only other individuals but also by shared resources. We first derive the model for the competitive spread of two viruses with an infrastructure network, and then provide conditions to ensure that the disease-free equilibrium (DFE) is globally exponentially stable under homogeneous and heterogeneous spread. For the design of efficient control strategies, we prove the exponential eradication of viruses in the case of switching between two types of spreading behavior, i.e., lockdown versus unrestricted movement. We then conclude with simulations that illustrate and confirm our theoretical results, along with an example of a possible lockdown method. The simulations with periodic infection rates display interesting unproven behavior, which can be the basis for future work.

KEYWORDS

Epidemic processes, competitive virus spread, time-varying networks, exponential stability

1 | INTRODUCTION

Mathematical modeling of disease spread has been an active area of research for more than two centuries, starting from Bernoulli's seminal paper that proposed a model for studying the benefits and risks of smallpox (Variola Major) vaccination[1]. The popularity of, and growing interest in, mathematical models for studying disease spread is absolutely unsurprising. Indeed, as Herbert Hethcote points out in[2], first of all, mathematical models, by virtue of the fact that they clearly state the assumptions involved, the values assigned to various parameters, etc. leave absolutely no room for ambiguity. As a result, an epidemiologist can obtain solid conceptual results (for instance, when does a virus get eradicated? when does it become endemic?) by leveraging such models. Secondly, one can, by effective use of computer simulations, check the efficiency of the various theoretical advancements obtained using the model under investigation. Moreover, one could also devise and check quantitative meaningful conjectures (for instance, can a given control policy achieve disease eradication within a given time-frame?), and also infer key model parameters from disease-specific data. Finally they contribute to the design and analysis of epidemiological surveys; suggest crucial data that should be collected, identify trends, and make general forecasts.[3]. As a consequence, mathematical models of disease spread significantly aid public health officials in not just combating an ongoing epidemic but also for improved preparedness against future outbreaks.

At the crux of it, mathematical modeling of disease spread relies on segregating the individuals in the given population into mutually exclusive health compartments; for instance, S (susceptible), I (infected), R (recovered), E (exposed), A (asymptomatic),

† The work of I.C. Morărescu and V.S.Varma was supported in part by the ANR through the grant NICETWEET ANR-20-CE48-0009. The work of Philip E. Paré was supported in part by the National Science Foundation, grants NSF-CNS #2028738 and NSF-ECCS #2032258.

etc. The combination of S, I and R compartments has spawned a plethora of models; notable among those being the susceptible-infected-susceptible (SIS) and the susceptible-infected-recovered (SIR) models. The present paper is focused on the SIS model. Observe that the spread of a disease need not be localized to an individual; it could, due to the ease of travel in the modern era, easily spread across multiple individuals. Hence, we focus our attention on *networked* SIS models, with each node in the network denoting an individual, and the interconnection among the nodes denoting the possible spreading pathways for the virus. The networked SIS model has been extensively studied[4,5,6].

A major drawback of the networked SIS models presented/studied in[5,7,8] is that these works implicitly assume that virus spread happens *only* due to person-to-person interaction. However, disease spread can also happen though media, such as grocery stores[9], transportation networks[10] and water distribution networks[11]. To underscore the issue at hand, note that in 1996 a group of scientists from the United States Center for Diseases and Control visited Uzbekistan, and conducted a study to identify the effects (if any) that water distribution systems have on the spread of cholera, with a view of providing water policy decisions in Nukus, Uzbekistan. Their empirical findings suggested that households that received (muncipal) piped water were more likely to contract diarrhea as compared to households that did not[11]. Thus, there is a pressing need for SIS models that also account for the possibility of the spread happening through multiple mediums. There has been partial progress in this direction: A networked susceptible-infected-water-susceptible (SIWS) model was proposed in[12]. The SIWS model in[12] was improved upon in[13] to account for the presence of an infrastructure *network*, as opposed to just a single infrastructure resource in[12]. Both[12,13] provide analytical results on the typical behaviors that the SIWS model exhibits. Nonetheless, their findings are restrictive, since the interconnection graph between the individuals is a static graph, and as such cannot deal with more complex scenarios. In particular, as seen during the recent COVID-19 crisis, individuals tend to move even when a pandemic is in full swing, which implies that the set of their neighbors possibly changes over time. Consequentially, the interconnection graph between the individuals needs to be *time-varying*. Thus, networked time-varying SIS models are needed.

Compared to the study of networked time-invariant SIS models, networked time-varying SIS models have received relatively less attention. This gap was partly rectified by the physics and community through the papers[14,15,16,17,18,19,20]. The findings in[14,15,16,17] have only been supported by simulations; none of these papers provide any rigorous analytical results, which negatively impacts our understanding of their behavior, and, consequently, our ability to make meaningful predictions about the dynamics of the system. The papers[21,22]are some of the earliest works to analytically describe the behavior of the time-varying continuous-time networked SIS model, while the papers[23,24] analyze a discrete-time version of the model presented in[21], under the assumption that the time-varying graph was a) periodic[24] or b) slowly-varying[23]. Although the paper[21] provides an in-depth understanding of virus spread over time-varying graphs, it suffers from two drawbacks: a) it does not account for the simultaneous spread of multiple (competing) viruses, and b) it does not account for the presence of a shared resource/infrastructure network. The possibility of simultaneous spread of multiple viruses (competing or otherwise) over a network coupled with the presence of an infrastructure network has non-trivial consequences, which stems from the fact that the dynamics of multi-virus spread is more richer than that of single-virus spread[25]. To better highlight the epidemiological complexities involved, consider the following scenario: It is possible for multiple lineages of avian influenza viruses to be simultaneously circulating in a population of birds. Furthermore, lineage A and lineage B, are known to be competitive, i.e., a bird infected with lineage A will, for the time duration that it is infected with said lineage, not be infected with lineage B[26]. Avian influenza viruses typically spread through loose contact with infected birds, and bodily fluid droplets. However, it has recently been observed that water bodies can also act as effective pathways for the spread of avian influenza. The aforementioned drawbacks are partly alleviated in[20], where a time-varying networked SIS model that factors in the presence of multiple competing viruses is proposed, although it does not account for the possibility of virus transmission over a shared infrastructure network. More recently, the model proposed in[27] overcomes the limitation of the modeling framework in[20], but does not account for the possibility of spread over *multiple* shared resource nodes, i.e., over a shared infrastructure network.

Our main contributions are as follows:

i) We present a model that accounts for the possibility of simultaneous spread of two competing viruses over a (time-varying) network of individuals and infrastructure network.
ii) We provide a suite of conditions for exponential convergence to the DFE, but under the assumption that the spread is homogeneous, and that the interconnection graph (among the individuals) is undirected; see Theorem 1.
iii) Building on Theorem 1 we identify a more general condition for exponential eradication of a virus, even when the interconnection graph is directed and the spread is not necessarily homogenous; see Theorem 2.
iv) The conditions in Theorem 1 and Theorem 2 require the state matrix, linearized around the DFE, to be Hurwitz for each time instant $t \in \mathbb{R}_{\geq \nu}$. In other words, in the aforementioned theorems we require that, with respect to a given virus $k \in [2]$,

the healing rate dominate the infection rate at all times for the eradication of virus k. Overcoming this restriction, we present yet another condition, where the linearized (in the sense above) state matrix needs to be Hurwitz only on average, for exponential eradication of a virus; see Theorem 3.

v) We design a control scheme that, by means of an appropriate choice of a switching rule, minimizes the time spent in lockdown while ensuring exponential eradication of a virus; see Proposition 1.

vi) Through numerical experiments, we shed light on conditions that might lead to both the viruses persisting in the network; in particular, we identify a scenario that might give rise to periodic behavior, such as limit cycles.

A preliminary version of this paper appeared in the proceedings of the 2022 European Control Conference[27]. The present paper differs from[27] in that the model in[27] only accounts for a) the spread of a single virus; and b) the presence of a *single* shared resource, as opposed to a network of shared resources. Consequently, Theorems 1, 2 and 3 are novel, and so is Proposition 1. Further, we provide complete proofs of all our results. Finally, we provide an in-depth set of simulations that not only illustrate our theoretical findings but also shed light on (some of) the possible endemic behavior that our model exhibits.

Paper Outline

The rest of the paper is organized as follows. We wrap up the present section by gathering all the notations that will be used in the sequel. Section 2 provides a detailed description of the model, which is followed by formal description of the main problems investigated in the present paper. Section 3 identifies a suite of conditions for exponential eradication of a virus, in a multi-virus setting, while a lockdown scheme for controlling disease spread is presented in Section 4. An in-depth set of simulations that illustrates not just our theoretical findings but also provides some experimental evidence of endemic behavior is included in Section 5. Finally, we summarize the paper, and provide some directions of future research that may be of possible interest to the wider Automatic Control community in Section 6.

Notation

Let $\mathbb{R}$, $\mathbb{R}_{\geq 0}$, and $\mathbb{N}$ denote the set of real numbers, nonnegative real numbers, and positive integers, respectively. For any positive integer n, we have $[n] = \{1, \ldots, n\}$. Given a matrix A, supposing its spectrum is real, $\lambda_1(A)$ denotes the maximum eigenvalue of A; the largest real-valued part of the eigenvalues of A is denoted by $r_1(A)$. We use $\mathbf{0}$ and $\mathbf{1}$ to denote the vectors whose entries all equal 0 and 1, respectively, and use I to denote the identity matrix, while the sizes of the vectors and matrix are to be understood from the context. For any two real matrices $A, B \in \mathbb{R}^{n\times m}$, we write $A \geq B$ if $A_{ij} \geq B_{ij}$ for all $i \in [n], j \in [m]$, and $A > B$ if $A \geq B$ and $A \neq B$.

2 | PROBLEM DESCRIPTION

2.1 | Model

Consider a network of n individuals, and suppose that there are two viruses, termed virus 1 and virus 2, circulating among the n individuals. Further, suppose that the aforementioned two viruses simultaneously spread also over an infrastructure network of q resource nodes. Assume that these viruses are competing; for an individual i, where $i \in [n]$, infection with virus 1 (resp. virus 2) precludes the possibility of simultaneous infection with virus 2 (resp. virus 1). We denote by β_i^k (resp. δ_i^k) the infection (resp. healing rate) of individual i with respect to virus k, while $A^k = [a_{ij}^k]_{n\times n}$, is the weighted time-varying adjacency matrix of the contact graph $G^k(t) = \{V, E^k(t)\}$ for the spread of virus k. In particular, for virus k, with $k \in [2]$, there is a one-to-one correspondence between the existence of a directed edge between nodes j and i, and corresponding entry in the matrix $A^k(t)$; $\{i, j\} \in E^K(t)$ if, and only if, $a_{ij}^k(t) > 0$, and moreover, $a_{ij}^k \geq 0$ denotes the strength of interconnection between nodes j and i for the spread of virus k. For brevity, we denote $\beta_{ij}^r(t) = \beta_i^r(t)a_{ij}^r(t)$. An individual could also get infected as a consequence of coming into contact with a contaminated resource in the infrastructure network. Let β_{ij}^{wk} denote the resource-to-individual infection rate for individual i from resource j for virus k. The spread of the k^{th} virus, where $k \in [2]$, in individual i can, therefore, be

represented as follows.

$$\dot{x}_i^k(t) = -\delta_i^k x_i^k(t) + \Big((1 - \textstyle\sum_{\ell=1}^{2} x_i^\ell(t)) \times \big(\textstyle\sum_{j=1}^{n} \beta_{ij}^k x_j^k(t) + \sum_{j=1}^{q} \beta_{ij}^{wk} w_j^k(t)\big)\Big), \tag{1}$$

where $w_j^k(t)$ denotes the concentration of virus k in resource j at time instant t. Note that $x_i^k(t)$ is an approximation of the probability of infection with respect to virus k of individual i at time instant t.

Viruses mutate over time. Additionally, it is not uncommon for people to move across towns or travel in general, even when an epidemic is ongoing. In order to account for both these possibilities we allow for the i) healing (resp. infection) rate for each individual to be time-varying; and ii) the set of neighbors that a node has to vary over time. Consequently, we need a more general form of (1), viz.

$$\dot{x}_i^k(t) = -\delta_i^k(t) x_i^k(t) + \Big((1 - \textstyle\sum_{\ell=1}^{2} x_i^\ell(t)) \times \big(\textstyle\sum_{j=1}^{n} \beta_{ij}^k(t) x_j^k(t) + \sum_{j=1}^{q} \beta_{ij}^{wk}(t) w_j^k(t)\big)\Big). \tag{2}$$

The concentration of the k^{th} virus in the j^{th} resource node at time t is governed by the following equation:

$$\dot{w}_j^k(t) = -\delta_j^{wk} w_j^k(t) + \textstyle\sum_{\ell=1}^{q} \alpha_{\ell j}^k w_\ell^k(t) - w_j^k(t) \sum_{\ell=1}^{q} \alpha_{j\ell}^k + \sum_{\ell=1}^{n} c_{j\ell}^{wk}(t) x_\ell^k(t), \tag{3}$$

where δ_j^{wk} denotes the healing rate of resource node j with respect to virus k; $\alpha_{j\ell}^k$ denotes the resource-to-resource infection rate for resource node ℓ from resource node j; and $c_{j\ell}^{wk}$ denotes the individual-to-resource infection rate for resource node j from individual ℓ.

The spread of the two viruses over a possibly time-varying population network and an infrastructure network can be represented using a time-varying graph. More specifically, we define a 2-layer graph $\mathcal{G}(t)$, where the vertices denote the individuals and the shared resource nodes, and layer k is the contact graph for the spread of virus k at time instant t, with $k \in [2]$. The rule for assigning an edge between two nodes in layer k, at time instant t, is as follows: At time instant t, there exists a directed edge from node j to node i in layer k, if, at time instant t, individual j (resp. shared resource ℓ, with $\ell \in [q]$) can infect individual i (resp. shared resource ℓ) with virus k. For ease of exposition, we define the following sets: $E^k(t) = \{(i,j) \mid i,j \in [n], a_{ji}^k(t) > 0\}$; $E_w^k = \{(\ell,j) \mid \ell,j \in [q], a_{\ell j}^k > 0\}$; $E_c^k(t) = \{(j,\ell) \mid \ell \in [n], j \in [q], c_{j\ell}^{wk}(t) > 0\}$; and $E_b^k(t) = \{(i,j) \mid i \in [n], j \in [q], \beta_{ij}^{wk}(t) > 0\}$. Finally, we define $\mathcal{E}^k(t) = E^k(t) \cup E_w^k \cup E_c^k(t) \cup E_b^k(t)$. Consequently, layer k of graph $\mathcal{G}$ at time t, denoted by $\mathcal{G}^k(t)$ is as follows: $\mathcal{G}^k(t) = (V, \mathcal{E}^k(t))$, with $|V| = n + q$.

In vector form, equations (2) and (3) can be written as follows:

$$\dot{x}^k(t) = ((I - \textstyle\sum_{\ell=1}^{2} X^\ell(t)) B^k(t) - D^k(t)) x^k(t) + (I - \textstyle\sum_{\ell=1}^{2} X^\ell) B_w^k w^k(t) \tag{4}$$

$$\dot{w}^k(t) = -D_w^k w^k(t) + A_w^k w^k(t) + C_w^k(t) x^k(t). \tag{5}$$

First define:

$$D_k(t) \coloneqq \begin{bmatrix} \delta_1^k(t) & 0 & \cdots & 0 \\ 0 & \delta_2^k(t) & \cdots & 0 \\ \vdots & \vdots & \ddots & \vdots \\ 0 & 0 & \cdots & \delta_n^k(t) \end{bmatrix}, \; B_k(t) \coloneqq \begin{bmatrix} \beta_{11}^k & \beta_{12}^k & \cdots & \beta_{1n}^k \\ \beta_{21}^k & \beta_{22}^k & \cdots & \beta_{2n}^k \\ \vdots & \vdots & \ddots & \vdots \\ \beta_{n1}^k & \beta_{n2}^k & \cdots & \beta_{nn}^k \end{bmatrix},$$

$$B_w^k(t) \coloneqq \begin{bmatrix} \beta_{11}^{wk} & \beta_{12}^{wk} & \cdots & \beta_{1q}^{wk} \\ \beta_{21}^{wk} & \beta_{22}^{wk} & \cdots & \beta_{2q}^{wk} \\ \vdots & \vdots & \ddots & \vdots \\ \beta_{n1}^{wk} & \beta_{n2}^{wk} & \cdots & \beta_{nq}^{wk} \end{bmatrix}, \; X^\ell(t) \coloneqq \begin{bmatrix} x_1^\ell(t) & 0 & \cdots & 0 \\ 0 & x_2^\ell(t) & \cdots & 0 \\ \vdots & \vdots & \ddots & \vdots \\ 0 & 0 & \cdots & x_n^\ell(t) \end{bmatrix}.$$

$$D_w^k \coloneqq \begin{bmatrix} \delta_1^{wk} & 0 & \cdots & 0 \\ 0 & \delta_2^{wk} & \cdots & 0 \\ \vdots & \vdots & \ddots & \vdots \\ 0 & 0 & \cdots & \delta_q^{wk} \end{bmatrix}, \; C_w^k \coloneqq \begin{bmatrix} C_{11}^{wk} & C_{12}^{wk} & \cdots & C_{1n}^{wk} \\ C_{21}^{wk} & C_{22}^{wk} & \cdots & C_{2n}^{wk} \\ \vdots & \vdots & \ddots & \vdots \\ C_{q1}^{wk} & C_{q2}^{wk} & \cdots & C_{qn}^{wk} \end{bmatrix},$$

$$A_w^k \coloneqq \begin{bmatrix} \alpha_{11}^k - \sum_{\ell=1}^q \alpha_{1\ell}^k & \alpha_{12}^k & \cdots & \alpha_{1q}^k \\ \alpha_{21}^k & \alpha_{22}^k - \sum_{\ell=1}^q \alpha_{2\ell}^k & \cdots & \alpha_{2q}^k \\ \vdots & \vdots & \ddots & \vdots \\ \alpha_{q1}^k & \alpha_{q2}^k & \cdots & \alpha_{qq}^k - \sum_{\ell=1}^q \alpha_{q\ell}^k \end{bmatrix}. \tag{6}$$

Next, define the following:

$$y^k(t) \coloneqq \begin{bmatrix} x^k(t) \\ w^k(t) \end{bmatrix}, \; X(y^k(t)) \coloneqq \begin{bmatrix} \mathrm{diag}(x^k(t)) & 0 \\ 0 & 0 \end{bmatrix},$$

$$\mathrm{B}_f^k(t) \coloneqq \begin{bmatrix} B^k(t) & B_w^k(t) \\ C_w^k(t) & A_w^k - \mathrm{diag}(A_w^k) \end{bmatrix}, \quad \text{and } D_f^k(t) \coloneqq \begin{bmatrix} D^k(t) & 0 \\ 0 & D_w^k - \mathrm{diag}(A_w^k) \end{bmatrix}.$$

Therefore, system (4)-(5) can be more compactly written as:

$$\dot{y}^k(t) = \left(-D_f^k(t) + (I - \textstyle\sum_{\ell=1}^2 X(y^\ell))B_f^k(t)\right) y^k(t), \tag{7}$$

with $k = 1, 2$. System (7) is referred to as the *continuous-time time-varying multi-competitive layered networked SIWS model*. Disease-spread models that account for the spread of competitive viruses and/or factor in the impact caused by spread through additional pathways such as an infrastructure network has been studied previously in, among others,[12,28,29,30]. It turns out system (7) has close connections to models studied in the aforementioned papers as we discuss in the following remarks.

Remark 1. By setting $A_w = \mathbf{0}$, (7) coincides with the model in[30], provided the model in[30] is specialized for the case of bivirus competitive spread.

Remark 2. Suppose that there is just one virus circulating in the population. Then

i) if $q = 1$, the model in system (7) is the same as the model in[28];
ii) if $a_{ij}(t) = a_{ij}$ for all $t \in \mathbb{R}_{\geq 0}$, the model in (7) is the same as the one in[31]; and
iii) assuming $A_w = \mathbf{0}$, and $a_{ij}(t) = a_{ij}$ for all $t \in \mathbb{R}_{\geq 0}$, and $q = 1$, (7) is the same as the model in[12].

Remark 3. Setting $w^k(t) = \mathbf{0}$ for $k = 1, 2$, and assuming there is only a single-virus spreading in the network, (7) collapses to the continuous-time time-varying networked SIS model studied in[21].

It is straightforward to see that, for $k = 1, 2$, if $x^k = \mathbf{0}$, and $w^k = \mathbf{0}$, then none of the nodes are infected by either of the viruses nor is there any contamination in the network of shared resources. We call this equilibrium the *disease-free equilibrium* (DFE).

With system (7) in place, the problems being studied in the present paper are as follows.

i) Assuming that, for each $k \in [2]$, the k^{th} layer of graph $\mathcal{G}(t)$ is, for each t, symmetric (i.e., $a_{ij}^k(t) = a_{ji}^k(t)$), and that $\beta_i(t) = \beta(t)$ for all $i \in [n]$ and for each t, identify a sufficient condition such that $y^k(t)$ converges to $\mathbf{0}$ exponentially fast.
ii) Accounting also for (possibly) directed graphs in the k^{th} layer of $\mathcal{G}(t)$, and also heterogeneous spread, i.e., there exists $i, j \in [n]$ and a time instant t_0 such that, for some $k \in [2]$, $\beta_i^k(t_0) \neq \beta_j^k(t_0)$, identify a sufficient condition such that $y^k(t)$ converges to $\mathbf{0}$ exponentially fast.

iii) Devise a lockdown procedure such that virus k, $k = 1, 2$, gets eradicated in finite time so as to ensure that critical health constraints are not violated. Thus, for a given initial time t_0 and $y^k(t_0)$, we want to ensure that

$$\|y^k(t)\| \leq \exp(-\lambda_0(t-t_0))\gamma\|y^k(t_0)\|, \tag{8}$$

for all $t \geq t_1$, for some finite $t_1 \geq t_0$ and $\gamma > 0$.

We require the following assumptions on the model parameters.

Assumption 1. Suppose that, for each $t \in \mathbb{R}_{\geq 0}$ and $k \in [2]$, $\delta_i^k(t) > 0$ for each $i \in [n]$, and $\delta_j^{wk}(t) > 0$ for each $j \in [q]$. Suppose that, for each $t \in \mathbb{R}_{\geq 0}$, and $k \in [2]$, $\beta_{ij}^k(t) \geq 0$ for all $i, j \in [n]$; for $i \in [n], j \in [q]$, $\beta_{ij}^{wk}(t) > 0$; and for $\ell \in [n], j \in [q]$, $c_{j\ell}^{wk}(t) > 0$.

Since we are interested in identifying sufficient conditions for exponential eradication of virus k, the following definition will be needed in the sequel.

Definition 1. Consider a system, described as follows:

$$\dot{x}(t) = f(t, x(t)), \tag{9}$$

where $f : \mathbb{R}_{\geq 0} \times \mathbb{R}^n \to \mathbb{R}^n$ is locally Lipschitz. The origin is a GES equilibrium point of (9) if there exist positive constants α and η, with $0 \leq \eta < 1$, such that

$$\|x(t)\| \leq \alpha \, \|x(t_0)\| \, \eta^{(t-t_0)}, \quad \forall \, t, t_0 \geq 0, \forall \, x(t_0) \in \mathbb{R}^n.$$

Since each x_i represents an approximation of the probability that individual i gets infected with virus k, it is immediate that the initial value of x_i^k is in $[0, 1]$, because otherwise the value of x_i^k will not correspond to physical reality. Similarly, it is also natural to assume that the initial value of w_j^k measured, for instance, in milligrams per litre is nonnegative. Consequently, we can say that the healthy state of virus k is exponentially stable if the condition in Definition 1 is satisfied for all $x_0^k \in [0, 1]^n$ and $w_j^k(0) \geq 0$, which implies that we can narrow our analysis to the set:

$$\mathcal{D}^k \coloneqq \{y^k(t) : x^k(t) \in [0, 1]^n, \, w^k(t) \in [0, \infty)^q\}. \tag{10}$$

Virus k is eradicated if $y^r(k) = \mathbf{0}$. The continuous-time multi-competitive layered networked SIWS model is in the *disease-free equilibrium* (DFE) if $y^r(k) = 0$, $\forall k \in [2]$.

The following lemma establishes that the set $\mathcal{D}^k$ is positively invariant.

Lemma 1. Consider system (7) under Assumption 1. If, for some $k \in [2]$, $x_i^k(0) \in [0, 1]$ for all $i \in [n]$, and $w_j^k(0) \geq 0$ for all $j \in [q]$, then $x_i^k(t) \in [0, 1]$ for all $i \in [n]$, and $w_j^k(t) \geq 0$, $\forall t \geq 0$.

Proof: Suppose that, for some $k \in [2]$ and arbitrary $i \in [n], j \in [q]$, at time $\tau \in \mathbb{R}_{\geq 0}$, we have that $x_i^k(\tau) = 0$, and $w_j^k(\tau) \geq 0$. Therefore, from (1), since by Assumption 1 $\beta_{ij}^k(t) > 0$ and $\beta_{ij}^{wk}(t) > 0$, $\dot{x}_i^k(\tau) \geq 0$. If $x_i^k(\tau) = 1$, then from (1), since by Assumption 1 $\delta_i^k(t) > 0$, $\dot{x}_i^k(\tau) < 0$. Putting the two cases together, it follows that, assuming $w_j^k(\tau) \geq 0$, $x_i^k(t) \in [0, 1]$ for all $t \geq \tau$. Since the choice of node i is arbitrary, it follows that, for all $i \in [n]$, $x_i^k(t) \in [0, 1]$ for all $t \geq \tau$. Next we show that, if, for some $j \in [q]$, and for the same τ as above, $w_j^k(\tau) \geq 0$, then $w_j^k(t) \geq 0$ for all $t \geq \tau$. Suppose that $w_j^k(\tau) = 0$. Then, from (3), since by Assumption 1, for all $\ell \in [n], j \in [q]$, $c_{j\ell}^{wk}(t) > 0$ for all $t \in \mathbb{R}_{\geq 0}$, and since we have already shown that $x_i(t) \in [0, 1]$ for all $t \geq \tau$, it follows that $\dot{w}_j^k(\tau) \geq 0$. Since the choice of node j was arbitrary, the same argument applies for all $j \in [q]$, which implies that $w_j^k(t) \geq 0$ for all $t\tau$, and $j \in [q]$. Observe that, by setting $\tau = 0$, we fulfill the hypothesis of the lemma, and, therefore, the claim follows. ■

3 | EXPONENTIAL ERADICATION OF VIRUS K

In this section, we identify sufficient conditions for GES of the DFE. We first consider the case where the spread is homogeneous (i.e., all agents have the same infection rate, for all time instants) and the underlying graph is symmetric and undirected, then we consider the case where the spread could also be heterogeneous (i.e., not all of the agents have the same infection rate for all time instants) and the underlying graph could also be directed.

3.1 | Homogeneous case

We consider the case where each node has the same infection rate, i.e., $\beta_i(t) = \beta(t)$ for all $i \in [n]$, and for all $t \in \mathbb{R}_{\geq 0}$. Furthermore, we assume that the interconnection graph, represented by the matrix $A(t)$, is undirected, and has symmetric weights, i.e., for each $t \in \mathbb{R}_{\geq 0}$, $a_{ij}(t) = a_{ji}(t)$. We have the following result, which is partly inspired from [21, Theorem 1].

Theorem 1. Consider system (7) under Assumption 1. Suppose that, for some $k \in [2]$, for each $t \in \mathbb{R}_{\geq 0}$, $\beta_i^k(t) = \beta(t)$ for all $i \in [n]$, $A^k(t), B_w^k(t), C_W^k(t)$, $D^k(t)$ and $D_w^k(t)$ are piecewise continuous in t, and bounded. Suppose that, for each $t \in \mathbb{R}_{\geq 0}$, $A^k(t) = A^k(t)^\top$, and $B_w^k(t) = C_w^k(t)$. If $\sup_{t\geq 0} \lambda_1(-D_f^k(t) + B_f^k(t)) < 0$, then the eradicated state of virus k is exponentially stable, with domain of attraction containing $\mathcal{D}^k$.

Proof: Consider an arbitrary $y^k(t) \geq 0$. For ease of notation, we will drop the time index in the rest of the proof. Define the Lyapunov function $V(y^k) = \frac{1}{2}(y^k)^\top y^k$. Observe that $V(y^k) = 0$ if, and only if, $y^k = \mathbf{0}$. For $y^k \neq \mathbf{0}$, we have:

$$
\begin{aligned}
\dot{V}(y^k) &= (y^k)^\top \dot{y}^k \\
&= (y^k)^\top \big(-D_f^k(t) + (I - X(y^k))B_f^k(t)\big) y^k \\
&= (y^k)^\top \begin{bmatrix} -D^k(t) + (I - X^k)B^k(t) & (I - X^k)B_w^k(t) \\ C_w^k(t)^\top & -D_w^k(t) + A_w^k \end{bmatrix} y^k \\
&\leq (y^k)^\top \begin{bmatrix} -D^k(t) + B^k(t) & B_w^k(t) \\ C_w^k(t)^\top & -D_w^k(t) + A_w^k \end{bmatrix} y^k \qquad (11) \\
&= (y^k)^\top \big(-D_f^k(t) + B_f^k(t)\big) y^k \qquad (12) \\
&\leq \lambda_1(-D_f^k(t) + B_f^k(t))||y^k||^2 \qquad (13) \\
&\leq \big(\sup_{t\geq 0} \lambda_1(-D_f^k(t) + B_f^k(t))\big)||y^k||^2 \qquad (14) \\
&< 0.
\end{aligned}
$$

Observe that, due to Assumption 1, for each $t \in \mathbb{R}_{\geq 0}$, $B^k(t)$, $B_w^k(t)$, and $C_w^k(t)$ are nonnegative. Since, by Lemma 1, $x_i^k(t) \in [0, 1]$ for each $i \in [n]$, and for all t, it follows that $(I - X)B(t) < B(t)$, and hence we obtain inequality (11). By assumption, for each $t \in \mathbb{R}_{\geq 0}$, $A^k(t) = A^k(t)^\top$, $\beta_i^k(t) = \beta(t)$ for each $i \in [n]$, and $B_w^k(t) = C_w^k(t)^\top$. Therefore, the matrix $(-D_f^k(t) + B_f^k(t))$ is symmetric, and by applying Rayleigh-Ritz Quotient [32] to (12), inequality (13) is immediate, while from the definition of supremum we obtain inequality (14). Since, by assumption, $\sup_{t\geq 0} \lambda_1(-D_f^k(t) + B_f^k(t)) < 0$, we obtain the final inequality. Since each of $B^k(t)$, $B_w^k(t)$, $C_w^k(t)$, $D^k(t)$ and $D_w^k(t)$ is piecewise continuous in t, and bounded, it follows that $-D_f^k(t) + B_f^k(t)$ is piecewise continuous in t, and bounded. Due to boundedness, the system is locally Lipschitz in y^k for all t, $y^k \geq \mathbf{0}$. Exponential eradication of virus k then follows from [33, Theorem 8.5]. ■

3.2 | Heterogeneous case

In this subsection, we study the case where the infection rates could possibly be different for some (all) nodes; the interconnection graph is not necessarily undirected. Our main finding, which is partly inspired from [34], is as follows.

Theorem 2. Consider system (7) under Assumption 1, with $B_f^k(t)$ and $D_f^k(t)$, for $k = 1, 2$, to be continuously differentiable. Suppose that, for some $k \in [2]$,

i) there exists $L > 0$ such that $\|B_f^k(t) - D_f^k(t)\| \leq L \; \forall t$;
ii) for some $\alpha_1 > 0$ $\sup_{t\geq 0} r_1(B_f^k(t) - D_f^k(t)) < -\alpha_1$; and
iii) there exists $\kappa > 0$ such that $\sup_{t\geq 0} \| \frac{d}{dt} \big(B_f^k(t) - D_f{}^k(t)\big)\| < \kappa$.

If κ is sufficiently small, then the eradicated state of virus k is exponentially stable, with domain of attraction containing $\mathcal{D}^k$.

The proof technique is closely related to that of [21, Theorem 2] and [35]; in the interest of completeness, the details are provided here.

Proof: Per the theorem hypothesis, for some $k \in [2]$, there exists $\alpha_1 > 0$, such that $\sup_{t\geq 0} r_1(B_f^k(t) - D_f^k(t)) < -\alpha_1$. Therefore, $\sup_{t\geq 0} r_1(B_f^k(t) - D_f^k(t)) < 0$. Hence, from the definition of supremum, it must be that, for each $t \in \mathbb{R}_{\geq 0}$, $r_1(B_f^k(t) - D_f^k(t)) < 0$, which further implies that, for each $t \in \mathbb{R}_{\geq 0}$, the matrix $(B_f^k(t) - D_f^k(t))$ is Hurwitz. Therefore, from [33, Theorem 4.12] it follows that, for each t, there exists a positive definite matrix $Q^k(t)$ such that

$$Q^k(t)(B_f^k(t) - D_f^k(t)) + (B_f^k(t) - D_f^k(t))^\top Q^k(t) = -I. \tag{15}$$

The solution to (15) is, then, given by

$$Q^k(t) = \int_0^\infty e^{(B_f^k(t)-D_f^k(t))^\top \tau} e^{(B_f^k(t)-D_f^k(t))\tau} d\tau. \tag{16}$$

Consider the possible Lyapunov function $V(y^k, t) = (y^k)^\top Q^k(t) y^k$. Since $Q^k(t)$ is, for each t, positive definite, it is clear that $V(y^k, t) > 0$ for all $y^k \neq \mathbf{0}$, and for all $t \geq 0$. Since $Q^k(t)$ is positive definite, for all t $Q(t)$ is symmetric, by definition. Moreover, since $Q^k(t)$ is an integration of product of matrix exponentials, and by noting that the first term in a power series expansion of a matrix exponential is the identity matrix I_{n+q}, it follows that $I_{n+q} \leq Q^k(t)$ for all $t \geq 0$. This implies that $\|y^k\|^2 \leq V(y^k, t)$.
Since conditions i) and ii) are, by assumption, satisfied, from [34] it follows that there exists a constant m, that depends on L and α_1 such that

$$\|e^{B_f^k(t)-D_f^k(t)\tau}\| \leq m \cdot e^{-\alpha_1 \tau} \quad \forall \tau \geq 0. \tag{17}$$

Hence, from (16) and (17) we obtain

$$\|Q^k(t)\| \leq \frac{m^2}{2\alpha_1}. \tag{18}$$

Since $Q^k(t)$ is symmetric for all $t \in \mathbb{R}_{\geq 0}$, by applying the Rayleigh-Ritz Quotient (RRQ) Theorem [32] we have:

$$\lambda_{\min}(Q^k(t))I \leq Q^k(t) \leq \lambda_{\max}(Q^k(t))I,$$

which implies

$$\begin{aligned}
\lambda_{\min}(Q^k(t))|y^k||^2 &\leq (y^k)^\top Q^k(t) y^k \\
&\leq \lambda_{\max}(Q^k(t))|y^k||^2 \\
&\leq ||Q^k(t)|| \cdot |y^k||^2 \qquad (19)\\
&\leq \frac{m^2}{2\alpha_1}|y^k||^2, \qquad (20)
\end{aligned}$$

where (19) follows from [32, Theorem 5.6.9], and (20) is due to (18). Combining with the lower bound on $V(y, t)$ obtained previously, we have the following:

$$\|y^k\|^2 \leq V(t, y^k) \leq \frac{m^2}{2\alpha_1}\|y^k\|^2, \tag{21}$$

Taking the time derivative of $V(y^k, t)$, we obtain

$$\begin{aligned}
\dot{V}(y^k, t) &= (y^k)^\top \dot{Q}^k(t) y^k + (y^k)^\top Q^k(t)\dot{y}^k + (\dot{y}^k)^\top Q^k(t) y^k \\
&= (y^k)^\top \dot{Q}^k(t) y^k + (y^k)^\top Q^k(t)\big(-D_f^k(t) + (I - X(y^k))B_f^k(t)\big) y^k \\
&\quad + (y^k)\top\big(-D_f^k(t) + B_f^k(t)^\top (I - X(y^k))\big) Q^k(t) y^k \qquad (22)\\
&\leq (y^k)^\top \dot{Q}^k(t) y^k + (y^k)^\top \Big[Q^k(t)(B_f^k(t) - D_f^k(t)) + (B_f^k(t) - D_f^k(t)^\top Q^k(t)\Big] y^k \qquad (23)\\
&= -\|y^k\|^2 + (y^k)^\top \dot{Q}^k(t) y^k, \qquad (24)
\end{aligned}$$

where inequality (23) comes from the fact that, since, by Assumption 1, $B_f^k(t)$ is nonnegative for each t, and by Lemma 1, $x_i^k(t) \in [0, 1]$ for each $i \in [n]$, and for all t, thereby implying that $(I - X(y^k))B_f^k(t) < B_f^k(t)$, while (24) is due to (15).

Differentiating $Q(t)$ with respect to time, we obtain the following:

$$\dot{Q}^k(t)(B_f^k(t) - D_f^k(t)) + Q^k(t)(\dot{B}_f^k(t) - \dot{D}_f^k(t)) + (B_f^k(t) - D_f^k(t))^\top \dot{Q}^k(t) + (\dot{B}_f^k(t) - \dot{D}_f^k(t))^\top Q^k(t) = 0. \tag{25}$$

Define

$$S^k(t) := (\dot{B}_f^k(t) - \dot{D}_f^k(t))^\top Q^k(t) + Q^k(t)(\dot{B}_f^k(t) - \dot{D}_f^k(t)). \tag{26}$$

Therefore, in view of (26), equation (25) can be rewritten as

$$\dot{Q}^k(t)(B_f^k(t) - D_f^k(t)) + (B_f^k(t) - D_f^k(t))^\top \dot{Q}^k(t) = -S^k(t). \tag{27}$$

The solution to (27) is, then, given by

$$\dot{Q}^k(t) = \int_0^\infty e^{(B_f^k(t)-D_f^k(t))^\top \tau} S^k(t) e^{(B_f^k(t)-D_f^k(t))\tau} d\tau. \tag{28}$$

Taking norms on both sides of (28) we get

$$\begin{aligned}
\|\dot{Q}^k(t)\| &= \| \int_0^\infty e^{(B_f^k(t)-D_f^k(t))^\top \tau} S^k(t) e^{(B_f^k(t)-D_f^k(t))\tau} d\tau \| \\
&= \int_0^\infty \| e^{(B_f^k(t)-D_f^k(t))^\top \tau} S^k(t) e^{(B_f^k(t)-D_f^k(t))\tau} \| d\tau && (29) \\
&\leq \int_0^\infty \| e^{(B_f^k(t)-D_f^k(t))^\top \tau} \| \| S^k(t) \| \| e^{(B_f^k(t)-D_f^k(t))\tau} \| d\tau && (30) \\
&= \|S^k(t)\| \int_0^\infty \| e^{(B_f^k(t)-D_f^k(t))^\top \tau} \| \| e^{(B_f^k(t)-D_f^k(t))\tau} \| d\tau && (31) \\
&= \|S^k(t)\| \|Q^k(t)\| && (32) \\
&\leq \frac{m^2}{2\alpha_1} \|S^k(t)\| && (33) \\
&\leq \frac{m^4}{4\alpha_1^2} \|\dot{B}_f^k(t) - \dot{D}_f^k(t)\|, && (34)
\end{aligned}$$

where (29) comes from replacing the norm of the integral by integral of the norm, (30) comes from submultiplicativity of matrix norms, and (32) comes from (16). The inequality (33) is a direct consequence of (17), whereas inequality (34) comes from taking norms on both sides of equation (26), and, again, leveraging the upper bound on the norm of $Q^k(t)$ in (17).

Plugging the inequality in (34) back into (24), we obtain the following:

$$\dot{V}(y^k, t) \leq (-1 + \frac{m^4}{4\alpha_1^2} \|\dot{B}_f^k(t) - \dot{D}_f^k(t)\|) \|y^k\|^2. \tag{35}$$

By assumption, there exists $\kappa > 0$ such that $\sup_{t\geq 0} \| \frac{d}{dt} \left(B_f^k(t) - D_f^k(t) \right) \| < \kappa$. Consequently, (35) could be rewritten as

$$\dot{V}(y^k, t) \leq (-1 + \frac{m^4}{4\alpha_1^2} \kappa) \|y^k\|^2. \tag{36}$$

Observe that choosing $\kappa = \frac{2\alpha_1^2}{m^4}$ results in $\dot{V}(y^k, t) \leq -\frac{1}{2}\|y^k\|^2$, which further implies that $\dot{V}(y^k, t) < 0$. Consequently, together in view of (21), from [33, Theorem 4.10] it follows that the eradicated state of virus k is exponentially stable with a domain of attraction including $\mathcal{D}^k$, thus concluding the proof. ■

Remark 4. Particularized to the setting without a shared resource, the difference between Theorem 2 and [21, Theorem 2] is as follows: Theorem 2 does not assume the existence of a constant that upper bounds the Lyapunov function $V(y, t)$; it turns out that the existence of such a constant is a direct consequence of the first two conditions in Theorem 2 being satisfied. The result [21, Theorem 2], to the contrary, assumes that such a constant exists and is well-defined, and together with conditions in Theorem 2 establishes exponential convergence to the DFE. Therefore, even particularized to the setting without a shared resource, Theorem 2 is more general than [21, Theorem 2].

Remark 5. Assuming that the first two conditions in Theorem 2 are satisfied, then the third condition in Theorem 2 may be slightly relaxed while still guaranteeing that the eradicated state of virus k is exponentially stable regardless of the initial

infection levels with respect to virus k[36]:

$$\int_t^{t+T} \|\dot{B}_f^k(s) - \dot{D}_f^k(s)\| ds \leq \mu T + \eta, \ \forall t \geq 0, \ \forall T \geq 0, \tag{37}$$

where $\eta > 0$ is some scalar, and μ depends on L and α_1.

Note that both Theorem 2, and its relaxation in Remark 5, require $B_f^k(t)$ and $D_f^k(t)$ to be continuously differentiable. For linear time-varying systems, a sufficient condition for global exponential stability (GES) of the origin that does not insist on the state matrix being continuously differentiable has been identified in [37, Theorem 3], while [38, Theorem 1] establishes GES of the origin even when the time-varying state matrix has fast variations (where fast is suitably defined). More recently, the authors in [38] have extended their findings for non-linear time-varying systems with fast variations in [39]; the stability guarantees therein are only semi-global. Generalizing [37, Theorem 3] and/or [38, Theorem 1] to also account for nonlinear time-varying systems of the kind in (7) is beyond the scope of the present paper, and is left for future work.

Note that Theorems 1 and 2 insist on the matrix $-D_f^k(t) + B_f^k(t)$ being Hurwitz for *each* $t \geq 0$. Consequently, verifying the conditions in Theorems 1 and 2 is extremely non-trivial. As such, we are interested in seeking less restrictive sufficient condition(s). Towards this end, we need the following assumption.

Assumption 2. Suppose that, for some $k \in [2]$,

i)

$$\lim_{T\to\infty} \frac{1}{T} \int_{t_0}^{t_0+T} \|-D_f^k(s) + B_f^k(s)\| ds \leq \alpha < \infty, \forall t_0 \geq 0. \tag{38}$$

ii) for some $v > 0$, there exists an $h > 0$ such that

$$\|-D_f^k(t+h) + B_f^k(t+h) + D_f^k(t) - B_f^k(t)\| \leq v h^\gamma, \tag{39}$$

for all $t \geq 0$, and for some γ such that $0 < \gamma \leq 1$.

iii)

$$\frac{1}{T} \int_{t_0}^{t_0+T} r_1(-D_f^k(s) + B_f^k(s)) ds \leq \bar{\sigma}, \tag{40}$$

for all $t_0 \geq 0$, $T \geq T_0$ and for some $\bar{\sigma} < 0$ and $T_0 > 0$.

Theorem 3. Consider system (7) under Assumptions 1 and 2. The eradicated state of virus k is exponentially stable, with domain of attraction containing $\mathcal{D}^k$, and

$$\|y^k(t)\| \leq \exp(-\lambda_0(t-t_0))\gamma \|y^k(t_0)\|, \tag{41}$$

for all $t \geq t_1$, for some finite $t_1 \geq t_0$ and $\lambda_0, \gamma > 0$.

Proof: Note that, by Assumption 1, $B_f^k(t)$ is, for all $t \in \mathbb{R}_{\geq 0}$, nonnegative. Since by Lemma 1, for each $i \in [n]$, $x_i(t) \in [0, 1]$ for all $t \geq 0$, it follows that $(I - \sum_{k=1}^2 X(y^k))B_f^k(t) < B_f^k(t)$. Therefore, system (7) can be bounded from above by the linear system

$$\dot{y}^k(t) = (-D_f^k(t) + B_f^k(t))y^k(t). \tag{42}$$

Consequently, by Gronwall's inequality [40], the solution of (7) will be bounded from above by the solution of the linear system (42). Observe that inequality (40) implies

$$\lim_{T\to\infty} \frac{1}{T} \int_{t_0}^{t_0+T} r_1(-D_f^k(s) + B_f^k(s)) ds \leq \bar{\sigma}, \tag{43}$$

for some negative scalar $\bar{\sigma}$, and for all $t_0 \geq 0$. Particularizing the result in [41, Theorem 2] for the case with no perturbation, inequalities (38), (39) in Assumption 2 together with inequality (43) imply that system (42) is GES. The existence of constants $\lambda_0 > 0$ and $\gamma > 0$ such that (41) is fulfilled follows from [41]. Hence, system (7) is GES, and (41) holds, thus concluding the proof. ■

4 | CONTROL STRATEGIES FOR AN EFFICIENT LOCKDOWN

We study the case in which two viruses are controlled by a lockdown procedure. In its natural state, i.e., without a lockdown, we consider that the population behaves in such a way that for all $k \in [2]$,

$$\sup_{t \geq t_0} r_1(B_w^k(t) - D_w^k(t)) < \bar{\sigma}_N^k, \tag{44}$$

for all $t_0 \geq 0$, with $\bar{\sigma}_N^k > 0$.We define $\bar{\sigma}_N = \max\{\bar{\sigma}_N^1, \bar{\sigma}_N^2\}$. However, during lockdown, the behavior for the population is such that Assumption 2 is satisfied and for all $k \in [2]$,

$$\frac{1}{T}\int_{t_0}^{t_0+T} r_1(-D_w^k(s) + B_w^k(s))ds \leq \bar{\sigma}_L^k, \tag{45}$$

for all $t_0 \geq 0$, with $\bar{\sigma}_L^k < 0$ as long as $T \geq T_{\min}^k$, with $T_{\min}^k > 0$ known. We define $\bar{\sigma}_L = \max\{\bar{\sigma}_L^1, \bar{\sigma}_L^2\}$ and $T_{\min} = \max\{T_{\min}^1, T_{\min}^2\}$.

Assuming that switching between the two strategies preserves the properties (38)-(39), our goal is to find a switching rule which ensures that all the conditions in Assumption 2 are satisfied, and therefore, by Theorem 3, guarantees the DFE is GES.

For any given t_0, let us first denote the sequence of switching times by $\{t_\ell, \ell \in \mathbb{N}\}$. We assume that switching to a lockdown mode and switching to a free mode (no lockdown) is done at

$$t_{2\ell} \text{ and } t_{2\ell+1}, \ \ell \in \mathbb{N}, \tag{46}$$

respectively.

We also assume that the lockdown is initiated at t_0 in order to control the epidemic.

Proposition 1. *Suppose Assumption 1,* (38)*,* (39)*,* (44)*, and* (45) *hold. If the lockdown switching sequence* $\{t_\ell, \ell \in \mathbb{N}\}$*, defined in* (46)*, is chosen such that* $t_{2\ell+1} - t_{2\ell} \geq T_{min}$*,* $\forall \ell \in \mathbb{N}$ *and*

$$\sum_{\ell=0}^{H} (\bar{\sigma}_L(t_{2\ell+1} - t_{2\ell}) + \bar{\sigma}_N(t_{2\ell+2} - t_{2\ell+1})) \leq \bar{\sigma}, \tag{47}$$

for all $H \in \mathbb{N}$*, then the system converges to the DFE in exponential time such that*

$$\|y^k(t)\| \leq \exp(-\lambda_0(t - t_0))\gamma\|y^k(t_0)\|,$$

for all $t \geq t_1$*, for some finite* $t_1 \geq t_0$ *and* $\lambda_0, \gamma > 0$*.*

Proof: Note that for any $T \geq T_{\min}$ there exists a $H \in \mathbb{N}$ and a switching rule such that $t_{2H+1} < T \leq t_{2H+2}$. Then for all $k \in [2]$,

$$\int_{t_0}^{t_0+T} r_1(-D_w^k(s) + B_w^k(s))ds \leq \sum_{\ell=0}^{H} \Big(\int_{t_{2\ell}}^{t_{2\ell+1}} r_1(-D_w^k(s) + B_w^k(s))ds + \int_{t_{2\ell+1}}^{t_{2\ell+2}} r_1(-D_w^k(s) + B_w^k(s))ds \Big) \tag{48}$$

$$\leq \sum_{\ell=0}^{H} (\bar{\sigma}_L(t_{2\ell+1} - t_{2\ell}) + \bar{\sigma}_N(t_{2\ell+2} - t_{2\ell+1})) \tag{49}$$

$$\leq \bar{\sigma}, \tag{50}$$

where (48) holds by partitioning the integral into sections in which the lockdown is implemented or not, following the sequence of lockdown and free mode intervals in (46). Equality occurs when $T = 2H + 2$, but it is less than when $t_{2H+1} < T < t_{2H+2}$ since partitions up to t_{2H+2} are still considered. Thus, the second integral on the right-hand side of (48) is positive. Then, (49) holds by (44) and (45). Finally, (50) follows as a result of (47). We have thus ensured that (40) holds for all T, which are the switching

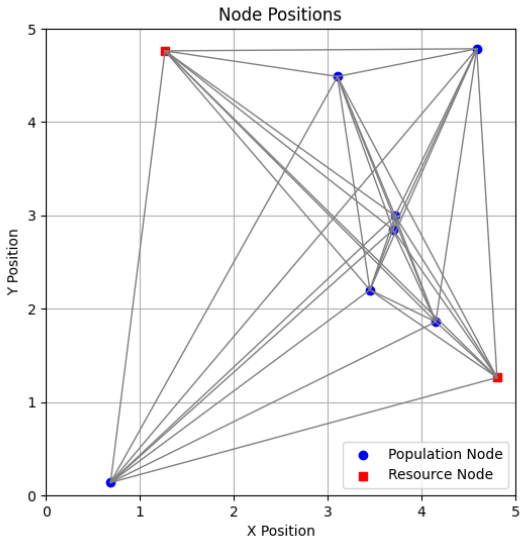

FIGURE 1 This plot shows the graph that the dynamics evolve over in the simulations. The position of each node was randomly generated. All of the simulations performed in Section 5.1 used the static graph shown above with edge weight calculated by (51)

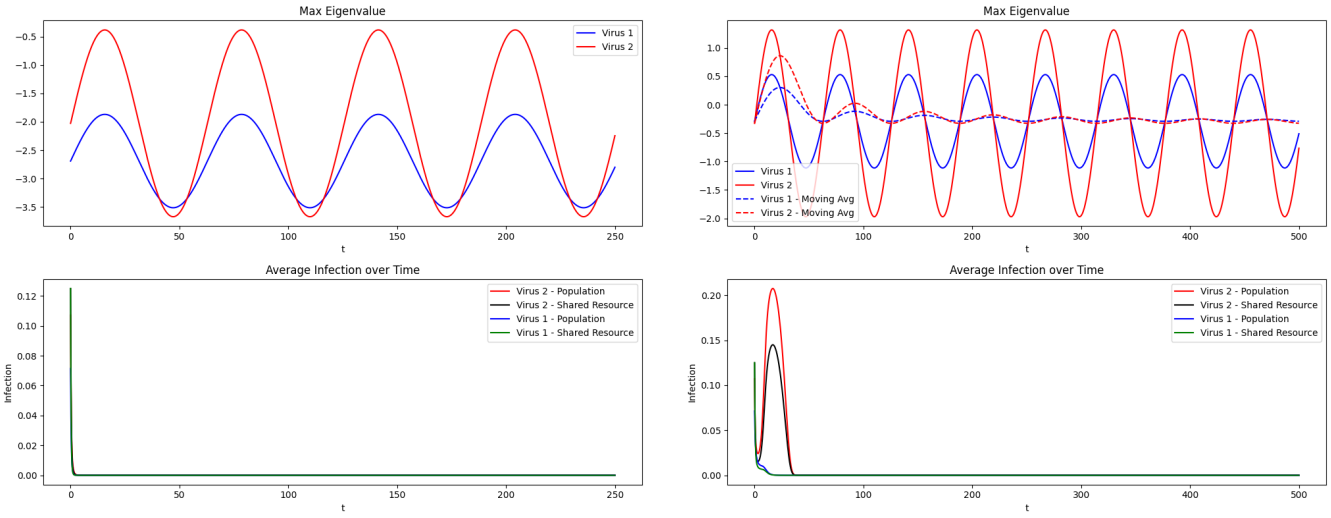

FIGURE 2 The simulation plots are of the maximum eigenvalue of $-D_f^k(t) + B_f^k(t)$ (above) and of the average infection level in the shared resource and population nodes in terms of virus 1 and virus 2 (below). In the left panel, the healing rates for virus 1 and virus 2 were $\delta_1 = 4.5$ and $\delta_2 = 4$, respectively. The infection rates were $\beta_1(t) = 1.1 + 0.5\sin(t/10)$ and $\beta_2(t) = 1.2 + \sin(t/10)$. In the right panel, the healing rates for virus 1 and virus 2 were $\delta_1 = 2.1$ and $\delta_2 = 2.3$, respectively. The time-varying infection rates for virus 1 and 2 were $\beta_1(t) = 1.1 + 0.5\sin(t/10)$ and $\beta_2(t) = 1.2 + \sin(t/10)$.

instants. Since we assumed (38) and (39) and have shown that the final requirement (i.e., (43)) in Assumption 2 is satisfied, the system will converge to the DFE in exponential time by Theorem 3. ■

Due to Proposition 1, we can minimize the time spent in lockdown as well as ensure an exponential convergence to the disease free equilibrium for all $t > t_0 + T_{\min}$ by selecting a switching rule that satisfies (47) with the inequality replaced by an equality. The details on how to do so are left for future work.

5 | SIMULATIONS

We now illustrate the analysis and control results via simulations. This section is organized as follows: First, we conduct simulations on a static graph with periodic infection rates, and subsequently on a dynamic graph with non-periodic time-varying infection rates. We also illustrate some interesting unproven behavior. The edge weights of each graph can be computed as follows:

$$a_{ij}(t) = \begin{cases} e^{-\|\chi_i(t)-\chi_j(t)\|^2}, & \text{if } \|\chi_i(t) - \chi_j(t)\| < r \\ 0, & \text{otherwise,} \end{cases} \tag{51}$$

where $\chi_i(t) \in \mathbb{R}^2$ is the position of node i and can change as a function of time. In the following subsection we explore simulations with a periodic infection rate where the graph is static, i.e., the node positions are not changing with time, thus the adjacency matrix is constant throughout the simulation.

5.1 | Periodic Infection Rates on Static Graphs

For the following simulations we have two viruses with periodic infection rates spreading over a static graph. The graph was created with randomized locations of seven population nodes and two shared resource nodes, as illustrated in Figure 1. The weight of each edge is computed in (51). Out of the nine nodes, three of them started with an initial infection level of 0.25 from virus 1, and another four began the simulation with an infection level of 0.25 from virus 2. The other two nodes had an initial infection value of 0 for both virus 1 and virus 2.

In the left panel of Figure 2, we see a simulation where the healing rates for virus 1 and virus 2 were $\delta_1 = 4.5$ and $\delta_2 = 4$, respectively, and the infection rates were $\beta_1(t) = 1.1 + 0.5\sin(t/10)$ and $\beta_2(t) = 1.2 + \sin(t/10)$. Note that in the top left plot of Figure 2 the supremum of the real part of the eigenvalue is always below zero for both viruses. Consequently, consistent with Theorem 1, we see that both viruses are eradicated in exponential time.

In the right panel of Figure 2, we see a simulation where the parameters were $\delta_1 = 2.1$, $\delta_2 = 2.3$, $\beta_1(t) = 1.1 + 0.5\sin(t/10)$, and $\beta_2(t) = 1.2 + \sin(t/10)$. The top right plot also includes a moving average of the maximum real part of the eigenvalue, which remains below zero after approximately 50 time steps. This behavior is also shown in the lower right plot of Figure 2 since both viruses are eradicated in exponential time, confirming Theorem 3.

In the left panel of Figure 3 the parameters were $\delta_1 = 0.21$, $\delta_2 = 0.15$, $\beta_1(t) = 1.1 + 0.5\sin(t/10)$, and $\beta_2(t) = 1 + \sin(t/10)$. We see that both viruses persist in the network in a periodic fashion. This behavior is also reflected in the average infection plot(bottom left). The simulation from the right panel in Figure 3 has parameters $\delta_1 = 0.21$, $\delta_2 = 0.2$, $\beta_1(t) = 1.1 + 0.5\sin(t/10)$, and $\beta_2(t) = 1.2 + \sin(t/15)$. This shift in the periods causes the plots of the maximum eigenvalue and average infection levels to shift as well. It is evident that the converse of Theorem 3 is illustrated by these simulations, since the average level of the maximum eigenvalue is greater than zero, and both viruses persist in the network. The cyclic properties seem to point to the existence of a limit cycle. This periodic behavior is common for influenza[42], and has also been observed with the most recent COVID-19 epidemic[43].

5.2 | Dynamic Graphs

Now we explore the behavior of the systems with dynamics graphs and viruses that are not periodic. The adjacency matrix is calculated from (51). For movement of the nodes, we assume piece-wise constant drift, confining the nodes to a fixed region. The positional dynamics of each node i are given by

$$\dot{\chi}_i(t) = \phi_i, \tag{52}$$

where $\phi_i \in \mathbb{R}^2$ with

$$\phi_{ik} = \begin{cases} -\phi_{ik}, & \text{if } z_k = z_{c_k} + l/2 \text{ or } z_k = z_{c_k} - l/2 \\ \phi_{ik}, & \text{otherwise,} \end{cases} \tag{53}$$

for each dimension $k = 1, 2$, where z_c is the center of a square that the nodes are bouncing around. In other words, if an agent arrives at a boundary of the box, the velocity of the agent in the corresponding dimension changes sign. Note that the simulation setup follows[21] except with the shared resource added. We set $b(t) = c(t)$. Also, note that, from (51), $A(t)$ is symmetric. While

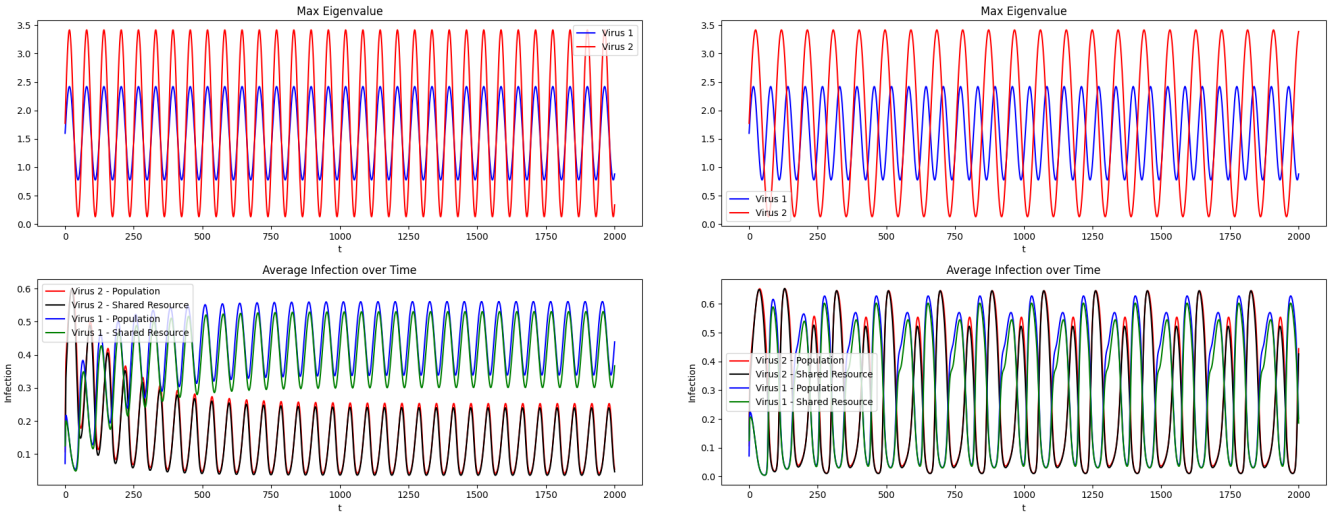

FIGURE 3 The simulation plots are of the maximum eigenvalue of $-D_f^k(t) + B_f^k(t)$ (above) and of the average infection level in the shared resource and population nodes in terms of virus 1 and virus 2 (below). In the left panel, the healing rates for virus 1 and virus 2 were $\delta_1 = 0.21$ and $\delta_2 = 0.15$, respectively. The time-varying infection rates for virus 1 and 2 were $\beta_1(t) = 1.1 + 0.5\sin(t/10)$ and $\beta_2(t) = 1 + \sin(t/10)$. In the right panel, the healing rates for virus 1 and virus 2 were $\delta_1 = 0.21$ and $\delta_2 = 0.2$, respectively. The infection rates were $\beta_1(t) = 1.1 + 0.5\sin(t/10)$ and $\beta_2(t) = 1.2 + \sin(t/15)$.

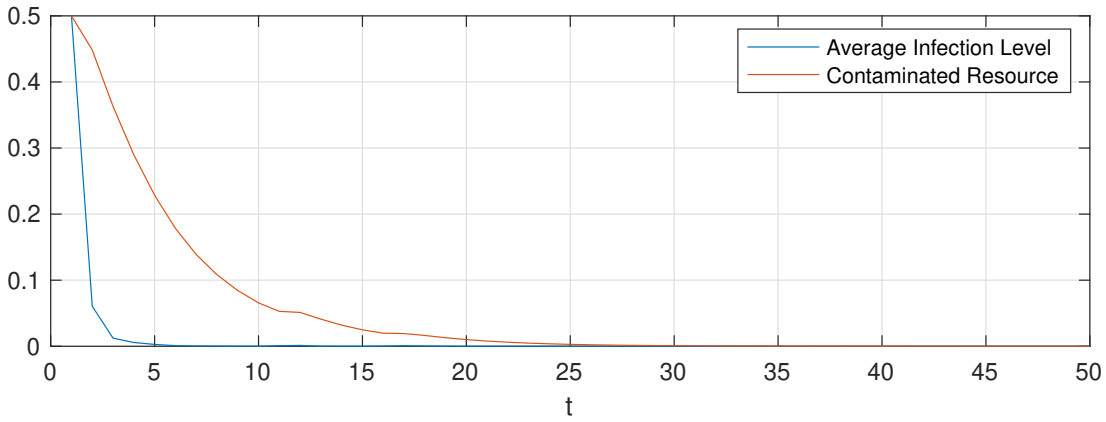

FIGURE 4 Average infection level ($\frac{1}{n}\sum_{i=1}^{n} x_i(t)$) and $z(t)$ in illustration of Theorem 1, with $\beta = 1$, $\delta = 3$, $\delta_w = 0.25$, and $z(0) = 0.5$.

these symmetry assumptions are only needed for Theorem 1, we factor the infection rates in a similar manner and employ the symmetric graph structure for simplicity in all the simulations.

For all the simulations we set $r = 10$. We assume there are 10 nodes ($n = 10$) that bounce around a box of dimension 5×5, centered at $z_c = (2.5, 2.5)$. A randomly infected set of nodes is initially infected ($x_i(0) = 1$). We assume time-invariant homogeneous viral spread, that is, the same β and δ for each node.

We first simulate a scenario that meets the assumptions of Theorem 1. We set $\beta = 1$, $\delta = 3$, and $\delta_w = 0.25$, and $z(0) = 0.5$. The average infection level ($\frac{1}{n}\sum_{i=1}^{n} x_i(t)$) and the resource contamination level ($z(t)$) are plotted in Fig. 4. The maximum eigenvalue for the simulation is plotted over time in Fig. 5. Note that the assumptions of Theorem 1 are met, with the largest eigenvalue always remaining below zero. Consistent with Theorem 1, the virus and the resource contamination die out quickly; see the blue line and red line, respectively.

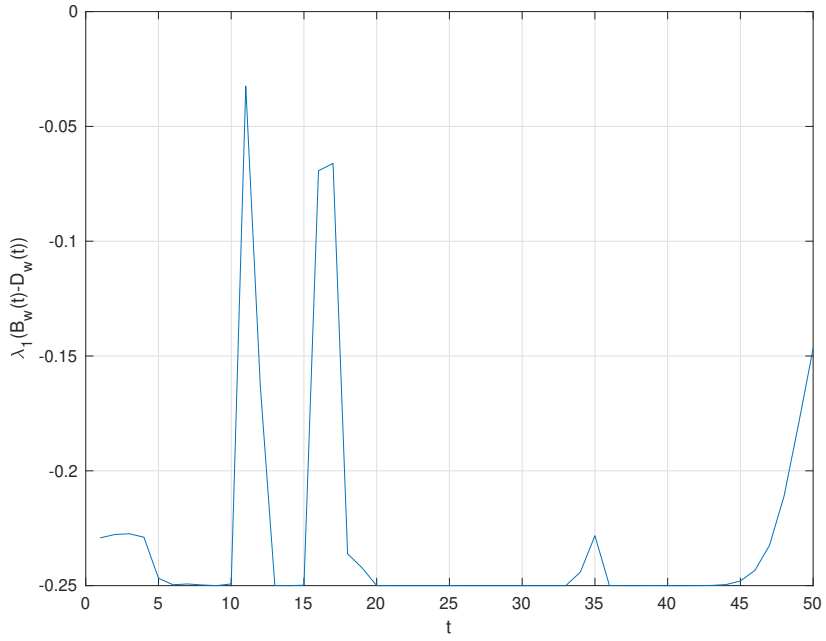

FIGURE 5 Maximum eigenvalue of the simulation in Fig. 4. Note that the maximum eigenvalue is always less than zero and the system converges to the DFE rapidly consistent with Theorem 1.

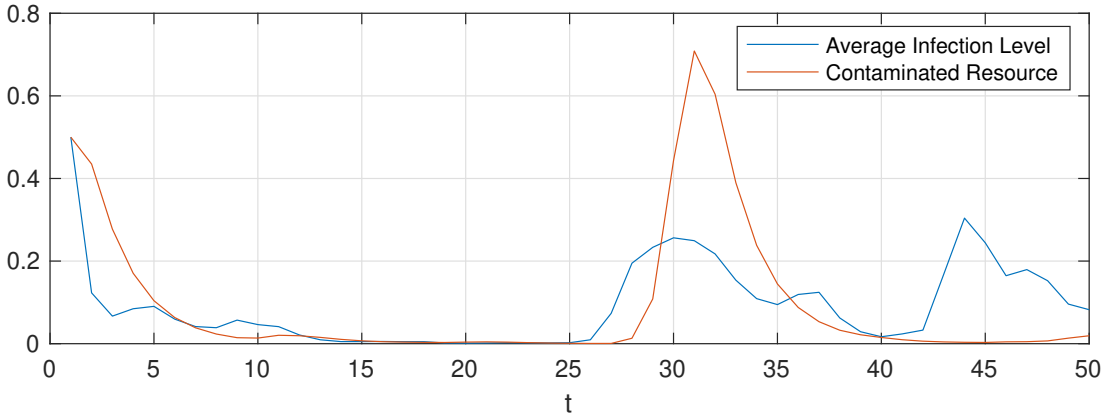

FIGURE 6 Average infection level and $z(t)$ in illustration of system with $\beta = 2$, $\delta = 2$, $\delta_w = 0.5$, and $z(0) = 0.5$. The lack of lockdown measures causes the infection level to rise rapidly around $t = 30$.

We also simulated a system that violated the assumptions of all the results. We set $\beta = 2$, $\delta = 2$, $\delta_w = 0.5$, and $z(0) = 0.5$. The average infection level and the resource contamination level are plotted in Fig. 6 with the corresponding maximum eigenvalues plotted over time in Fig. 7. Note that the eigenvalues are mostly greater than zero and the virus persists in the system.

In order to enact the on/off lockdown control policy proposed in Section 4, we devise the following social distancing protocol that is implemented for ten time steps. While not letting node i leave the square region,

$$\dot{\chi}_i(t) = \frac{\sum_{j,a_{ij}(t)>0.001} \chi_i - \chi_j}{\| \sum_{j,a_{ij}(t)>0.001} \chi_i - \chi_j \|}, \tag{54}$$

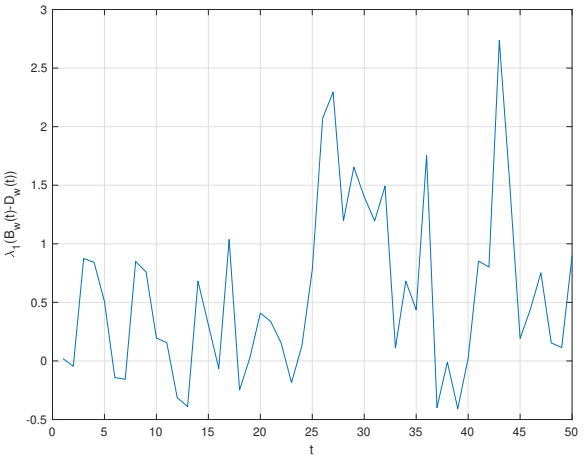

FIGURE 7 Maximum eigenvalue of the simulation in Fig. 6. Note that the maximum eigenvalue is greater than zero most of the time and the virus persists in the network (see Fig. 6).

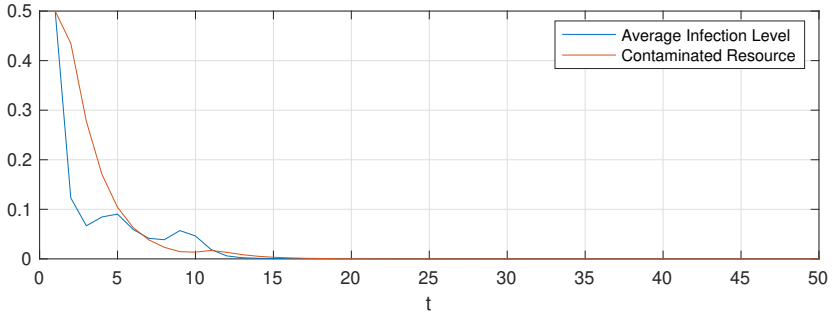

FIGURE 8 Average infection level and $z(t)$ in illustration of the endemic system from Fig. 6 with the social distancing policy from (54) every 20 time steps, starting at time $t = 10$. With the on/off lockdown strategy implementation added, the virus in Fig. 6 is eradicated.

forcing the nodes to separate from each other. We implement this algorithm every 20 time steps, starting at time $t = 10$, for the endemic system from Fig. 6. The average infection level and the resource contamination level are plotted in Fig. 8 with the corresponding maximum eigenvalues plotted over time in Fig. 9. Note that the eigenvalues are almost always less than zero, the 20-time step average is always below zero, and the virus no longer persists in the system, dying out quite quickly, consistent with the result in Proposition 1.

6 | CONCLUSION

In this paper, we developed a model that describes the dynamics of the spread of two competing viruses over a layered network comprising of individuals at one level, and resources at the other level. The key novelty of our model is that the graph describing the interconnection between the individuals is time-varying.We proved several theoretical results identifying conditions that are sufficient for the exponential eradication of viruses in the networks. To design efficient control strategies, we proved that switching between lockdown and unrestricted movement modes is a viable strategy to force the viruses to be exponentially eradicated. We also performed two different cases of simulations. The first set of simulations explore periodic infection rates on a static graph. Our simulations on periodic infection rates not only confirm our theoretical results, but also allude to the presence of a limit cycle. The second set of simulations explore non-periodic but time-varying infection rates on a dynamic graph. The

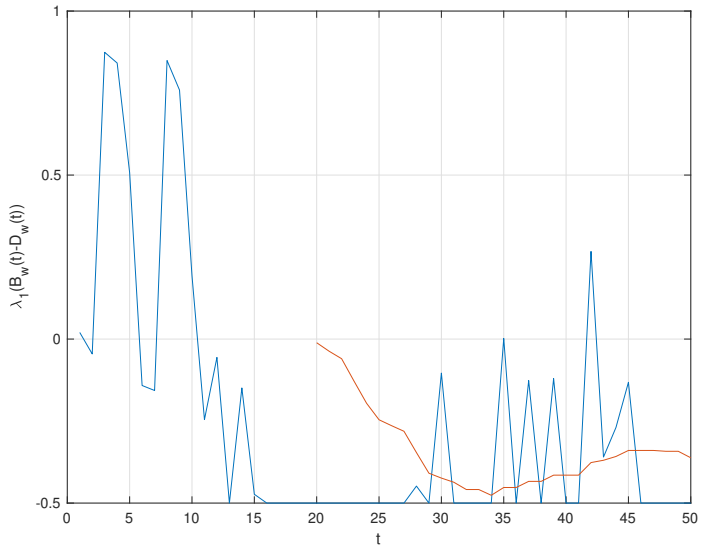

FIGURE 9 Maximum eigenvalue of the simulation in Fig. 8 plotted in blue and the 20-time step average plotted in red. Note that the average is always below zero, satisfying the conditions of Proposition 1; the control strategy eradicates the virus (see Fig. 8).

simulations on the dynamic graph showed that our proposed social distancing procedure is able to eradicate viruses exponentially and control the average infection levels in the networks. There are multiple directions for future work. One includes finding conditions that induce a limit cycle as illustrated in the simulations. Another direction for future work includes the design of optimal lockdown strategies.

References

1. Bernoulli D. Essai d'une nouvelle analyse de la mortalité causée par la petite vérole, et des avantages de l'inoculation pour la prévenir. *Histoire de l'Acad., Roy. Sci.(Paris) avec Mem* 1760: 1–45.

2. Hethcote HW. The mathematics of infectious diseases. *SIAM review* 2000; 42(4): 599–653.

3. Hethcote HW, Van Ark JW. Modeling HIV transmission and AIDS in the United States. *Lecture notes in Biomathematics* 1991; 95.

4. Lajmanovich A, Yorke JA. A deterministic model for gonorrhea in a nonhomogeneous population. *Mathematical Biosciences* 1976; 28(3-4): 221–236.

5. Khanafer A, Başar T, Gharesifard B. Stability of epidemic models over directed graphs: A positive systems approach. *Automatica* 2016; 74: 126–134.

6. Fall A, Iggidr A, Sallet G, Tewa JJ. Epidemiological models and Lyapunov functions. *Mathematical Modelling of Natural Phenomena* 2007; 2(1): 62–83.

7. Van Mieghem P, Omic J, Kooij R. Virus spread in networks. *IEEE/ACM Transactions on Networking (TON)* 2009; 17(1): 1–14.

8. Nowzari C, Preciado VM, Pappas GJ. Analysis and control of epidemics: A survey of spreading processes on complex networks. *IEEE Control Systems Magazine* 2016; 36(1): 26–46.

9. Mahoney FJ, Hoge CW, Farley TA, et al. Communitywide outbreak of Legionnaires' disease associated with a grocery store mist machine. *Journal of Infectious Diseases* 1992; 165(4): 736–739.

10. Nakata Y, Röst G. Global analysis for spread of infectious diseases via transportation networks. *Journal of mathematical biology* 2015; 70(6): 1411–1456.

11. Semenza JC, Roberts L, Henderson A, Bogan J, Rubin C. Water distribution system and diarrheal disease transmission: a case study in Uzbekistan.. *The American journal of tropical medicine and hygiene* 1998; 59(6): 941–946.

12. Liu J, Paré PE, Du E, Sun Z. A networked SIS disease dynamics model with a waterborne pathogen. In: IEEE. ; 2019: 2735–2740.

13. Paré PE, Janson A, Gracy S, Liu J, Sandberg H, Johansson KH. Multilayer SIS Model With an Infrastructure Network. *IEEE Transactions on Control of Network Systems* 2022; 10(1): 295–307.

14. Barrett CL, Bisset KR, Eubank SG, Feng X, Marathe MV. Episimdemics: an efficient algorithm for simulating the spread of infectious disease over large realistic social networks. In: IEEE. ; 2008: 1–12.

15. Vestergaard CL, Génois M. Temporal Gillespie algorithm: fast simulation of contagion processes on time-varying networks. *PLoS computational biology* 2015; 11(10): e1004579.

16. Sun K, Baronchelli A, Perra N. Contrasting effects of strong ties on SIR and SIS processes in temporal networks. *The European Physical Journal B* 2015; 88: 1–8.

17. Liu QH, Xiong X, Zhang Q, Perra N. Epidemic spreading on time-varying multiplex networks. *Physical review E* 2018; 98(6): 062303.

18. Prakash BA, Tong H, Valler N, Faloutsos M, Faloutsos C. Virus propagation on time-varying networks: Theory and immunization algorithms. In: Springer. ; 2010: 99–114.

19. Bokharaie V, Mason O, Wirth F. Spread of epidemics in time-dependent networks. In: . 5. IFAC. ; 2010.

20. Paré PE, Liu J, Beck CL, Nedić A, Başar T. Multi-competitive viruses over time-varying networks with mutations and human awareness. *Automatica* 2021; 123: 109330.

21. Paré PE, Beck CL, Nedić A. Epidemic processes over time-varying networks. *IEEE Transactions on Control of Network Systems* 2018; 5(3): 1322–1334.

22. Mason O, Wirth FR, Rami MA, Bokharaie V. Stability criteria for SIS epidemiological models under switching policies. *Discrete and Continuous Dynamical Systems Series* 2014; 19(9): 2865–2887.

23. Paré PE, Gracy S, Sandberg H, Johansson KH. Data-driven distributed mitigation strategies and analysis of mutating epidemic processes. *Proc. 59th IEEE Conference on Decision and Control,* 2020a: 6138–6143.

24. Gracy S, Paré PE, Sandberg H, Johansson KH. Analysis and distributed control of periodic epidemic processes. *IEEE Transactions on Control of Network Systems* 2020; 8(1): 123–134.

25. Newman ME. Threshold effects for two pathogens spreading on a network. *Physical Review Letters* 2005; 95(10): 108701.

26. Bahl J, Vijaykrishna D, Holmes EC, Smith GJ, Guan Y. Gene flow and competitive exclusion of avian influenza A virus in natural reservoir hosts. *Virology* 2009; 390(2): 289–297.

27. Gracy S, Morărescu IC, Varma VS, Paré PE. Analysis and On/Off Lockdown Control for Time-Varying SIS Epidemics with a Shared Resource. In: IEEE. ; 2021.

28. Gracy S, Morarescu IC, Varma VS, Paré PE. Analysis and on/off lockdown control for time-varying SIS epidemics with a shared resource. In: IEEE. ; 2022: 1660–1665.

29. Cui S, Liu F, Liang L, Jardón-Kojakhmetov H, Cao M. An SIS diffusion process with direct and indirect spreading on a hypergraph. *Automatica* 2025; 177: 112319.

30. Cui S, Liu F, Jardón-Kojakhmetov H, Cao M. Discrete-time layered-network epidemics model with time-varying transition rates and multiple resources. *Automatica* 2024; 159: 111303.

31. Paré PE, Janson A, Gracy S, Liu J, Sandberg H, Johansson KH. Multilayer SIS Model With an Infrastructure Network. *IEEE Transactions on Control of Network Systems* 2022; 10(1): 295–307.

32. Horn RA, Johnson CR. *Matrix Analysis*. Cambridge University Press . 2012.

33. Khalil HK. *Nonlinear Systems*. Prentice Hall. 3 ed. 1996.

34. Desoer C. Slowly varying system $\dot{x} = A(t)x$. *IEEE Transactions on Automatic Control* 1969; 14(6): 780–781.

35. Rosenbrook H. The stability of linear time-dependent control systems. *International Journal of Electronics* 1963; 15(1): 73–80.

36. Ioannou PA, Sun J. *Robust Adaptive Control*. Courier Corporation . 1996.

37. Gao X, Liberzon D, Liu J, Başar T. Unified stability criteria for slowly time-varying and switched linear systems. *Automatica* 2018; 96: 110–120.

38. Liberzon D, Shim H. Stability of linear systems with slow and fast time variation and switching. In: IEEE. ; 2022: 674–678.

39. Liberzon D, Shim H. Stability of nonlinear systems with slow and fast time variation and switching: The common equilibrium case. In: IEEE. ; 2024: 5622–5627.

40. Gronwall TH. Note on the derivatives with respect to a parameter of the solutions of a system of differential equations. *Annals of Mathematics* 1919: 292–296.

41. Solo V. On the stability of slowly time-varying linear systems. *Mathematics of Control, Signals and Systems* 1994; 7(4): 331–350.

42. Bjørnstad ON, Viboud C. Timing and periodicity of influenza epidemics. *Proceedings of the National Academy of Sciences* 2016; 113(46): 12899-12901. doi: 10.1073/pnas.1616052113

43. Manabe H, Manabe T, Honda Y, et al. Simple mathematical model for predicting COVID-19 outbreaks in Japan based on epidemic waves with a cyclical trend. *BMC Infectious Diseases* 2024; 24(465).